

Long-term climate-influenced land cover change in discontinuous permafrost peatland complexes

Olivia Carpino^{1*}, Kristine Haynes¹, Ryan Connon², James Craig³, Élise Devoie³ and William Quinton¹

5 ¹*Cold Regions Research Centre, Wilfrid Laurier University, Waterloo, Ontario, N2L 3C5, CANADA*

²*Environment and Natural Resources, Government of the Northwest Territories, Yellowknife, Northwest Territories, X1A 2L9, CANADA*

³*Department of Civil and Environmental Engineering, University of Waterloo, Waterloo, Ontario, N2L 3G1, CANADA*

10 *Corresponding author contact information: ocarpino@wlu.ca (519-884-1970)

Abstract

The discontinuous permafrost zone is undergoing rapid transformation as a result of unprecedented permafrost thaw brought on by circumpolar climate warming. Rapid warming over recent decades has significantly decreased the area underlain by permafrost in peatland complexes. It has catalyzed extensive landscape transitions in the Taiga Plains of northwestern Canada, transforming forest-dominated landscapes to those that are wetland-dominated. However, the advanced stages of this landscape transition, and the hydrological and thermal mechanisms and feedbacks governing these environments, are unclear. This study explores the current trajectory of land cover change across a 300,000 km² region of northwestern Canada's discontinuous permafrost zone by presenting a north-south space-for-time substitution that capitalizes on the region's 600 km latitudinal span. We combine extensive geomatics data across the Taiga Plains with ground-based hydrometeorological measurements collected in the Scotty Creek basin, Northwest Territories, Canada, which is located in the medial latitudes of the Taiga Plains and is undergoing rapid landscape change. This data is used to inform a new conceptual framework of landscape evolution that accounts for the observed patterns of permafrost thaw-induced land cover change, and provides a basis for predicting future changes. Permafrost thaw-induced changes in hydrology promote partial drainage and drying of collapse scar wetlands, leading to areas of afforestation forming treed wetlands without underlying permafrost. Across the north-south latitudinal gradient spanning the Taiga Plains, relatively undisturbed forested plateau-wetland complexes dominate the region's higher latitudes, forest-wetland patchworks are most prevalent at the medial latitudes, and forested peatlands are increasingly present across lower latitudes. This trend reflects the progression of wetland transition occurring locally in the plateau-wetland complexes of the Scotty Creek basin and informs our understanding of the anticipated trajectory of change in the discontinuous permafrost zone.

Keywords: discontinuous permafrost zone; Taiga Plains; peatland; climate change; boreal forest; hydrology; energy dynamics

Key Points

1. Conceptual framework developed to understand the trajectory of permafrost thaw-induced land cover change
2. Permafrost thaw-induced land cover change varies latitudinally across the plateau-wetland complexes of the discontinuous permafrost zone
3. Partial wetland drainage triggers ecohydrological and thermal feedbacks that promote reforestation after full permafrost thaw

40

1. Introduction

Northwestern Canada is one of the most rapidly warming regions on Earth (Vincent *et al.*, 2015; Box *et al.*, 2019) and it is transitioning to a warmer state at a rate that appears to have no analogue in the historical record (Porter *et al.*, 2019). This transition includes region-wide
45 thaw and disappearance of permafrost at unprecedented rates (Rowland *et al.*, 2010). The Taiga
Plains ecoregion of northwestern Canada extends from 55° to 68° N and as such, encompasses
the spectrum of permafrost cover, from continuous to sporadic. Permafrost thaw in the Taiga
Plains ecoregion is especially pronounced in its lower latitudes where the permafrost is relatively
thin and warm, often already at the thaw-point temperature (Biskaborn *et al.*, 2019), indicating a
50 state of disequilibrium with the current climate (Helbig *et al.* 2016a). For example, Kwong &
Gan (1994) repeated the permafrost surveys of Brown (1964) in northern Alberta and the
southern Northwest Territories (NWT) and found that the southern limit of permafrost
occurrence had migrated northward by about 120 km over a period of 26 years. Beilman &
Robinson (2003) estimated that 30-65% of the permafrost has disappeared from the southern
55 Taiga Plains in the preceding 150 years, most of which disappeared in the latter 50 years. The
accelerated rates of permafrost warming and thaw observed in recent decades throughout the
circumpolar region (Biskaborn *et al.*, 2019), including all of northwestern Canada (Kokelj *et al.*
2017; Holloway & Lewkowiz 2019), have dramatically transformed land covers in the southern
Taiga Plains (Chasmer & Hopkinson, 2017).

60 Much of the southern Taiga Plains is occupied by peatland-dominated lowlands, a
landscape of raised, black spruce (*Picea mariana*) tree-covered peat plateaus overlying thin (<10
m), ice-rich permafrost interspersed with permafrost-free, treeless wetlands. These permafrost-
free wetlands are predominantly classified as channel fens and collapse scar wetlands, the latter

of which is developed from thermokarst erosion of the plateaus (Robinson & Moore, 2000). Peat
65 plateaus and collapse scar wetlands are typically arranged into distinct “plateau-wetland
complexes,” which are separated by channel fans. Each of these major land cover types in the
lowlands of the southern Taiga Plains, have contrasting hydrological functions (Hayshi *et al.*,
2004) and therefore changes to their relative proportions on the landscape can affect water flux
and storage at the basin scale (Quinton *et al.*, 2011). Permafrost thaw underlying plateaus is
70 driven by horizontal conduction and advection from adjacent wetlands, and vertical heat flows
from the ground surface (Walvoord & Kurylyk, 2016). As this permafrost thaws, the overlying
plateau ground surface subsides and is engulfed by the surrounding wetlands (Beilman *et al.*,
2001; Quinton *et al.*, 2011; Helbig *et al.*, 2016a). As such, permafrost thaw in this environment
transforms forests to treeless, permafrost-free wetlands (Robinson & Moore, 2000). In the
75 process, this also changes the hydrological function of the transformed land cover, in part due to
a change in surface water-groundwater interactions (McKenzie & Voss 2013). Such a
transformation can profoundly affect local drainage processes and pathways (Connon *et al.* 2014;
2015) with implications to regional hydrology (St. Jacques & Sauchyn, 2009; Korosi *et al.* 2017;
Connon *et al.*, 2018), ecology (Beilman, 2001) biogeochemical processes (Gordon *et al.*, 2016)
80 and carbon cycling (Vonk *et al.*, 2019; Helbig *et al.* 2016a).

Zoltai (1993) described a perpetual cycle of permafrost development and thaw in which
permafrost evolves from perennial ice bulbs that form below *Sphagnum* hummocks in
permafrost-free treeless wetlands (*i.e.* collapse scars). Such hummocks expand and coalesce
eventually forming tree-covered plateaus. However, over time plateaus experience a disturbance
85 (*e.g.* fire, disease) that initiates the development of collapse scars and as a result, the plateau or
portions of it revert to a permafrost-free wetland. In a stable climate, the permafrost and
permafrost-free fractions of a landscape are assumed to remain relatively consistent. Zoltai

(1993) estimated that the time required to complete this cycle is approximately 600 years. Treat and Jones (2018) indicated time scales for forest recovery following permafrost thaw in the range of 450 to 1500 years. However, there is growing evidence throughout the southern Taiga Plains that the climate warming of recent decades has disrupted the cycle of permafrost thaw and redevelopment such that the rates of permafrost loss greatly exceed those of permafrost development (*e.g.* Halsey *et al.*, 1995; Robinson & Moore, 2002; Quinton *et al.*, 2011).

The accelerated rates of permafrost thaw and resulting land cover change described above call into question the utility of existing concepts (*e.g.* Zoltai, 1993) as a means to estimate the current trajectory of land cover change since such concepts were developed from analyses of geological sediments (*e.g.* peat cores) which generally lack the resolution needed to identify land cover change sequences over relatively short (*i.e.* decadal) periods. Moreover, it is uncertain whether the current rates of climate warming are represented in the sediment record. As a result, there remains considerable uncertainty on the trajectory of permafrost thaw-induced land cover change in this region, including possible end-members and intermediate stages. Because of the close connection between land cover type and hydrological function in this region, the uncertainty related to possible land cover change trajectories also raises new uncertainties in regards to the region's water resources.

In addition to unprecedented climate warming in the North, accelerated permafrost thaw is also driven by positive feedbacks including increased fragmentation of forested peat plateaus with increasing thaw (Chasmer *et al.*, 2011), a process which increases the length of interface between permafrost and permafrost-free terrain, and therefore also increases the overall flux of energy into the remaining permafrost bodies (Kurylyk *et al.*, 2016). Connon *et al.* (2018) demonstrated that talik layers situated between the active layer and underlying permafrost are

widespread in thawing peatland-dominated terrains and their occurrence increases with increasing permafrost thaw. Devoie *et al.* (2019) demonstrated that once a talik forms, the rate of permafrost thaw can increase 10-fold.

115 Since the permafrost table beneath peat plateaus rises above the water surface of the adjacent wetlands, plateaus function as “permafrost dams” that prevent wetlands from draining. Permafrost thaw therefore removes this effect and enables previously impounded wetlands to partially drain until the hydraulic gradient driving their partial drainage reaches an equilibrium state (Haynes *et al.*, 2020). The slow release of water from the long-term storage of wetlands no longer impounded by permafrost changes the physical and ecological characteristics and
120 hydrological function of these wetlands (Haynes *et al.*, 2020). Such drainage transforms the uniformly wet *Sphagnum* lawns that characterise impounded wetlands, into hummocky surfaces that provide a wider range of near surface moisture conditions including those sufficiently dry to support the re-growth of trees (Haynes *et al.*, 2020). There is also evidence that when black spruce forest is lost due to permafrost thaw and plateau inundation, forest regeneration does not
125 depend on the regeneration of permafrost (Haynes *et al.* 2020; Chasmer & Hopkinson 2017). For example, treeless collapse scars have transformed into black spruce forest within two to three decades after the permafrost dams disappear (Haynes *et al.* 2018).

In addition to the transient drainage process described above that may occur following the removal of the impounding permafrost (Haynes *et al.*, 2018), such removal also increases the
130 hydrological connectivity of basins through the incorporation of wetlands that were previously impounded and therefore hydrologically isolated from the basin drainage network (Connon *et al.*, 2015). This process of “wetland capture” expands the runoff contributing areas of basins, a process that increases their runoff potential. Connon *et al.* (2018) attributed the trends of

increasing runoff ratio (*i.e.* fraction of basin runoff per unit input of precipitation) in basins
135 throughout the Taiga Plains to this permafrost thaw-induced process of runoff contributing area
expansion.

The transition of one type of ground cover to another as a result of permafrost thaw or a
subsequent process such as partial wetland drainage and re-establishment of forest also results in
a change of surface energy balance (Kurylyk *et al.* 2016; Devoie *et al.* 2019). Insight into the
140 nature of such changes can be obtained through comparing the energy regimes of the existing
suite of land covers including the end-members of land cover change. For example, the incoming
solar radiation measured at a height of 2 m above the ground surface is highest in the treeless
wetlands and lowest in areas of peat plateaus with dense forest (Haynes *et al.*, 2019). The
average shortwave radiation flux density of treeless wetlands is approximately twice of that
145 measured below dense forest (Haynes *et al.*, 2019). Plateau areas with moderate or sparse tree
canopies have incoming solar radiation values intermediate between these two end members
(Chasmer *et al.*, 2011). The ground surface albedo varies over the narrow range of 0.15 to 0.19
(Hayashi *et al.*, 2007) among the ground surface types discussed here, the exception being the
late snowmelt period while plateau ground surfaces are still snow covered and the treeless
150 wetlands are snow-free (Disher *et al.* 2021; Connon *et al.*, Submitted).

The nature of changes to a land cover's surface energy balance is governed by the
properties of its subsurface, ground surface, and the overlying tree canopy, all of which change
as one land cover type transitions to another (Helbig *et al.* 2016b). The reduction in the areal
cover of forested plateaus and concomitant increase in the coverage of treeless wetlands
155 indicates that in the first instance, permafrost thaw increases the incoming shortwave flux to the
transformed land cover (Kurylyk *et al.* 2016; Devoie *et al.* 2019). Chasmer *et al.* (2011) found

that this thaw-induced transition and associated increase of incoming shortwave radiation occurs over several years as tree mortality decreases the density of tree canopies. However, the forests that subsequently re-establish in partially drained wetlands may have an energy balance that shares some characteristics of the forested peat plateaus, where insolation is relatively low, and the low albedo (and therefore high energy adsorption) of trunks, branches and stems result in relatively high long-wave and sensible heat compared to the treeless wetland surfaces (Helbig *et al.* 2016b).

Unprecedented climate warming and the feedbacks to thaw and land cover change are new factors not accounted for in current theories on permafrost degradation-aggregation cycles based on the analysis of peat cores. As a result, the time scales for land cover transformations derived from such theories cannot account for the current rates and patterns of all thaw-induced land cover change. This study examines peat plateau-wetland complexes along a latitudinal gradient through the Taiga Plains to improve the understanding of permafrost thaw-driven land cover change in this region as well as to advance the ability to predict land cover changes over the coming decades. This overall objective will be accomplished by: (1) delineating the current extent of peatlands and forest distribution along the latitudinal span of discontinuous permafrost; (2) characterising the end-members and intervening stages of land cover transition; (3) providing an interpretation of the hydrological and ground surface energy balance regimes for each stage of land cover transition based on twenty years of field studies at the Scotty Creek Research Station; and (4) presenting a conceptual framework of peatland transition during and following permafrost thaw.

2. Study Site

2.1 The Taiga Plains Ecozone

180 Much of northwestern Canada's boreal region is located within the discontinuous
permafrost zone, which ranges latitudinally from extensive-discontinuous (50-90% areal
permafrost coverage) in the north to sporadic-discontinuous (10-50%) in the south. Within this
region, the Taiga Plains ecozone contains a patchwork of mineral and organic terrain. This study
examines the peat plateau-collapse scar wetland complexes that dominate the lowlands of this
185 ecoregion (Wright *et al.* 2009; Helbig *et al.* 2016a). While air temperature is the predominant
control on permafrost, relatively dry peat at the ground surface can allow permafrost to exist
where mean annual air temperatures (MAATs) are at or even above 0°C due to thermal
insulation (Vitt *et al.* 1994; Camill & Clark 1998). Permafrost is therefore largely restricted to
below peat plateaus since only these features contain unsaturated layers sufficiently developed to
190 insulate permafrost (Zoltai & Tarnocai 1975; Hayashi *et al.* 2004; Quinton *et al.* 2009). The areal
coverage of permafrost in the discontinuous zone has significantly decreased in recent decades
due to increasing MAATs and has resulted in a shift towards more wetland-dominated
landscapes (Thie, 1974; Robinson & Moore, 2000; Wright *et al.* 2009; Quinton *et al.*, 2011;
Olefeldt *et al.* 2016).

195 The discontinuous permafrost zone of the Taiga Plains ecozone covers 312,000 km² and,
for the purposes of this study, is divided into the areas of extensive-discontinuous permafrost
(151,000 km²) and sporadic-discontinuous permafrost (161,000 km²) (Brown *et al.*, 2002; Figure
1). The Taiga Plains, bounded by the Taiga Cordillera to the west and Taiga Shield to the east,
has a dry continental climate with short summers and long, cold winters with MAATs ranging
200 from -5.5°C to -1.5°C (Vincent *et al.* 2012). MAATs have increased across the Taiga Plains over

the past 50 years (1970 – 2019) (Vincent *et al.* 2012) in a manner consistent with panarctic warming (Overland *et al.*, 2019). This is largely due to increases in average winter and spring temperatures of approximately 3°C over this period (Vincent *et al.* 2012). However, there has been no consistent trend in mean annual precipitation over this period in the Taiga Plains (Mekis & Vincent, 2011).

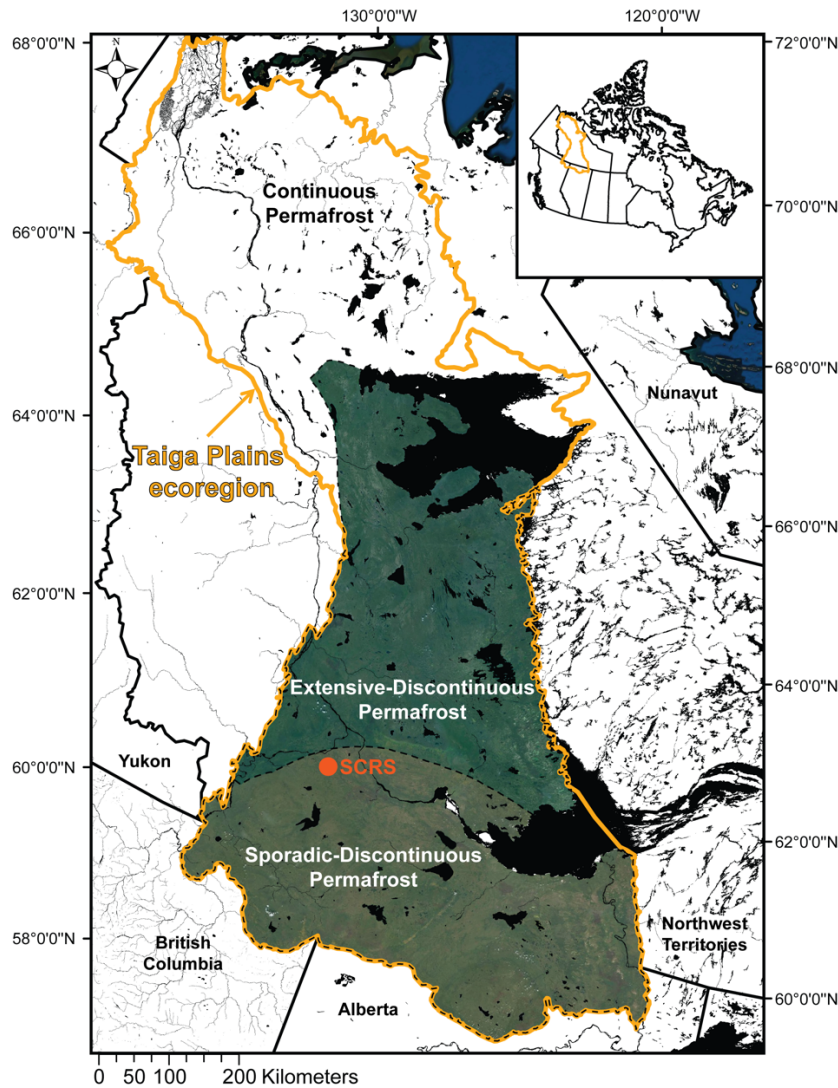


Figure 1: The Taiga Plains ecoregion with the discontinuous permafrost zones (coloured) defining the study region (Brown *et al.* 2002). The location of Scotty Creek Research Station (SCRS) is also indicated. Contains information licensed under the Open Government Licence – Canada.

2.2 Scotty Creek, Northwest Territories

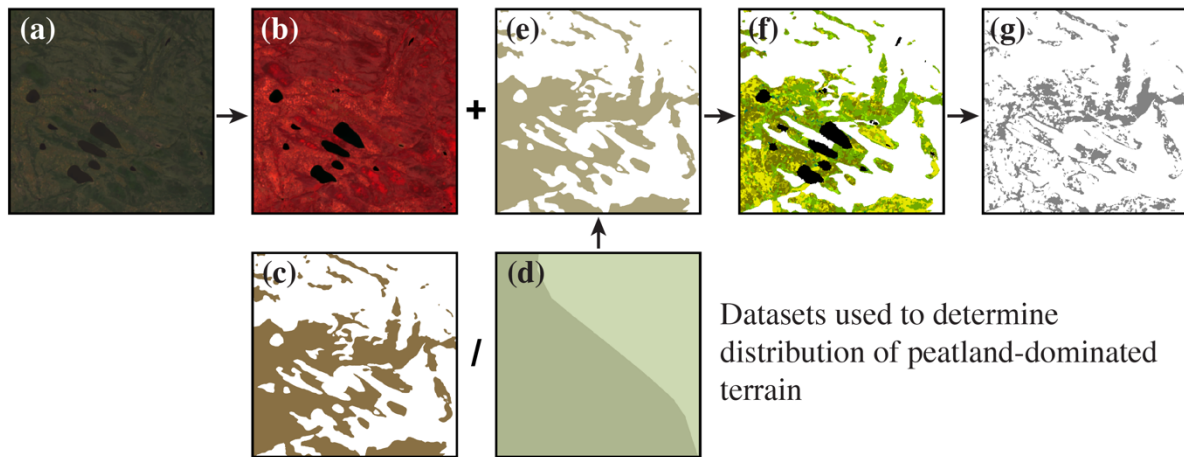
Scotty Creek (61.3°N, 121.3°W) has been the focus of field studies and monitoring since the mid-1990s and as such, the long-term and detailed data archive at Scotty Creek (Haynes *et al.*, 2019) provide a unique opportunity to evaluate land cover changes over a period that coincides with rapid climate warming. Scotty Creek therefore also provides a reference to interpret land cover changes for terrains that are also present throughout the region. Scotty Creek is located approximately 50 km south of Fort Simpson, Northwest Territories (Figure 1) where the MAAT (1970-2015) is -2.6°C and the mean annual precipitation (1970-2015) is 400 mm, of which 150 mm falls as snow (Environment and Climate Change Canada, 2019). Data collected by Environment and Climate Change Canada at the Fort Simpson A climate station show that MAAT has increased by approximately 0.05°C/year since 1950, with warming most pronounced during the winter. Scotty Creek drains a 152 km² area dominated by peatlands with peat accumulations ranging between 2 and 8 m overlying a clay and silt rich glacial till (McClymont *et al.*, 2013). The Scotty Creek drainage basin occupies one of many peatland-dominated lowlands of the Taiga Plains, and as such its landscape is dominated by complexes containing tree-covered peat plateaus overlying permafrost alongside treeless and permafrost free collapse scar wetlands. Such plateau-wetland complexes are separated by channel fens that collectively function as the basin drainage network (Hayashi *et al.* 2004; Quinton *et al.* 2009). This type of land cover not only dominates the lowlands of the Taiga Plains but is also found extensively throughout northwestern Canada and across the circumpolar subarctic (Olefeldt *et al.* 2016).

3. Methods

3.1 Geomatics Methods

To place Scotty Creek into a regional context, geomatics methods were applied to both
235 zones of discontinuous permafrost within the Taiga Plains to quantify the areas occupied by each
of the major land covers of all areas identified as peatland-dominated lowland. Multispectral
Landsat 8 imagery (30 m resolution; Figure 2a) was acquired across an area of over 300,000 km²
totalling 70 Landsat scenes. Of these, 59 scenes were used to construct the base of the mosaic
and 11 were used as secondary data to patch and minimize cloud cover. The 59 primary scenes
240 were acquired in 2017 and 2018 while the 11 secondary scenes were acquired between 2013 and
2016 as data of suitable quality was unavailable during the preferred time period. Acquiring
imagery during the snow-free season was prioritized and as such, all 70 Landsat tiles were
acquired in June, July, or August, rendering the coniferous forest cover seasonally comparable
and allowing for a more streamlined mosaicking process. A colour infrared mosaic (Landsat 8
245 bands 5, 4, 3 displayed as R, G, B; Figure 2b) was created across the study region in ArcGIS
(ESRI, Redlands, California) using a Lambert Conformal Conic projection. The mosaic dataset
was colour balanced and the boundary was amended to the Taiga Plains ecozone including the
delineations dividing the sporadic and extensive discontinuous zones (Brown *et al.* 2002).

Method to determine fractional forested area in peatland-dominated terrain



250 Figure 2: A summary of the regional geomatics methods used over a 2 km x 2 km sample
area. Two main workflows are highlighted: the datasets used to map probable peatland-
dominated terrain and the methods used to determine fractional forested area within those
peatland-dominated areas. (a) Multispectral Landsat 8 imagery; (b) false-colour infrared
255 Landsat 8 imagery; (c) Natural Resources Canada saturated soils dataset; (d) Northern
Circumpolar Soil Carbon Database (NCSCD) fractional area of organic soils; (e)
probable peatland-dominated terrain; (f) unsupervised classification identifying land
covers within peatland-dominated terrain; (g) coniferous forest cover within peatland-
dominated terrain.

260 To determine the current distribution of the peatland-dominated lowlands that contain the
same type of terrain as observed at Scotty Creek (*i.e.* plateau-wetland complexes separated by
channel fens), two complementary products were used in the ArcGIS suite of programs. First, a
Natural Resources Canada saturated soils dataset (Figure 2c; Natural Resources Canada 2017)
was selected to isolate areas that were wetland-dominated and likely representative of the
265 plateau-wetland complexes targeted in this study. Next, the Northern Circumpolar Soil Carbon
Database (NCSCD) (Figure 2d; Bolin Centre for Climate Research 2013) was selected to
determine whether the highlighted wetland-dominated areas are also likely to represent peatland-
dominated areas.

The saturated soils dataset is part of a larger digital cartographical project of Natural
270 Resources Canada, CanVec. The CanVec dataset is a vector format dataset, which can be

downloaded by province/territory or Canada-wide and includes over 60 features organized into 8 themes, including land features. Land features in this dataset, such as the distribution of saturated soils, were originally digitized at a scale of 1:50000 (Natural Resources Canada 2017). The NCSCD is also a polygon database developed by the Bolin Centre for Climate Research through synthesizing data from numerous regional and national soil maps alongside field-data collected across Canada, USA, Russia, and the European Union. The NCSCD includes data on the fractional coverage of different soil types and stored soil organic carbon (Hugelius *et al.* 2013a; Hugelius *et al.* 2013b). In the present study, the layer containing information on the fractional coverage of soil types was used. While the original format of the NCSCD is a vector of delineated zones, gridded data is also available at resolutions varying from 0.012° to 1° (Hugelius *et al.* 2013b). The NCSCD is comprised of a circumarctic dataset as well as country-wide and regional datasets, including one of Canada (Hugelius *et al.* 2013b).

The NCSCD is a widely used dataset (Olefeldt *et al.* 2014; Gibson *et al.* 2018; Stofferahn *et al.*, 2019; etc.) but the zones do not map specific locations of peatland-dominated terrain (Figure 2d). The locations of peatlands is helpful for work in regions such as the Taiga Plains, where the landscape is a patchwork of both organic and mineral terrain. The saturated soils dataset and the NCSCD were then both masked to the Taiga Plains boundaries in ArcGIS, where over 26,000 saturated soil polygons and 572 NCSCD zones were contained within the study region. The saturated soils dataset was mapped to display probable peatland terrain across the study region (Figure 2c). The areas of each saturated soil polygon were calculated alongside the areas for each NCSCD zone using the boundaries in the dataset. As the fractional coverage product from the NCSCD was used in this study, the fractional area of probable peatland terrain within the same NCSCD zone was calculated. The fractional areas of organic soils reported in

the NCSCD were then compared to the fractional areas of probable peatland terrain from the
295 saturated soils dataset within the same NCSCD zone boundary (Figure 2e).

The Landsat mosaic dataset (Figure 2b) was then combined with the resultant product
displaying peatland terrain (Figure 2e). An unsupervised land cover classification was
subsequently completed on the Landsat mosaic across the areas identified by the saturated soils
and NCSCD datasets to identify and classify the land covers within these peat plateau-wetland
300 complexes (Figure 2f). The first iteration of the unsupervised classification (Iso Cluster
classification approach) targeted 50-75 classes (72 created). The original 72 classes were then
aggregated into 12 final classes within the peatland terrain outlined across the Taiga Plains study
region. The final 12 aggregated classes include: coniferous (dense and sparse), mixed (dense and
sparse), and broad leaf forests stands (dense and sparse), collapse scar, fen, open water, bare
305 ground, cloud, and cloud shadow.

Forested peatlands are particularly indicative of landscape change in this region (Quinton
et al. 2010; Baltzer *et al.* 2014; Chasmer & Hopkinson 2017) and as such, identifying the
forested areas within the already identified peatland-dominated terrain was the focus of the
Landsat classification. Specifically, the proportion of coniferous forested area within the total
310 peatland area was quantified across the region's latitudinal span (Figure 2g). Fractional
coniferous forested area was selected rather than total forested area to account for the observed
spatial differences in peatland distribution across the Taiga Plains. For each degree of latitude, a
bin was created for fractional forested area and the median was calculated alongside upper (*i.e.*
75th percentile) and lower (*i.e.* 25th percentile) quartiles. This data was plotted as a function of
315 latitude across the Taiga Plains ecozone. This generated a dataset of forest cover across the

peatland-dominated regions of interest that was subsequently complemented by field data collected in the Scotty Creek basin to guide the proposed conceptual framework.

3.2 Scotty Creek Imagery

To help capture examples of the stages of the transitioning landscape, imagery was collected using a Remotely Piloted Aircraft System (RPAS) across the Scotty Creek basin to represent how each of these illustrated trajectory stages manifests on the landscape in a peat plateau and collapse scar wetland-dominated environment. The RPAS imagery (0.5 m resolution) was collected in the summer of 2018 using an eBee Plus equipped with a senseFly SODA 3D mapping camera and all image processing was completed in Pix4DMapper.

Imagery for Scotty Creek, including aerial photographs from 1947, 1970, and 1977, IKONOS satellite imagery from 2000, and Worldview satellite imagery from 2010 and 2018 were used to quantify the area occupied by peat plateaus, collapse scar wetlands and channel fens in each of these years. The aerial photographs (0.5-1.2 m resolution) and IKONOS imagery (4 m resolution) were previously classified and the results were presented in Quinton *et al.* (2011). Carpio *et al.* (2018) completed the land cover classifications for the 2010 Worldview imagery and Disher (2020) classified the 2018 Worldview imagery. Collectively, these images document the land cover change at the Scotty Creek basin over the period 1947 to 2018.

3.3 Hydrological Data

A comprehensive archive of hydrometeorological measurements was used in this study to examine the temporal variation in hydrological characteristics as land cover transition from one stage to another. The form and hydrological function of the major land cover types of permafrost plateau, collapse scar, and channel fen are well understood from numerous studies at Scotty Creek since the 1990s (Quinton *et al.* 2019). Field studies and monitoring at Scotty Creek over

340 this period have also provided firsthand accounts of how permafrost thaw changes land covers
(Quinton *et al.* 2019). In the present study, we examined how runoff, evapotranspiration, and
water storage are affected as land cover changes. In addition, we examined the precipitation data
collected from 2008 to 2019 (Geonor, Model T200B) in relation to the three hydrological
components listed above to gain insights into how changes in land cover affect the water balance
for each stage in the land cover transition. These stages will be presented in detail in section 4.2.
345 The Geonor precipitation data include both rain and snow measurements logged at 30 minute
intervals (Table 1). Monitoring of discharge from Scotty Creek by the Water Survey of Canada
began in 1996. For this study, annual basin runoff (mm year^{-1}) between 1996 and 2015 was
calculated and used in the basin runoff component of the conceptual framework (Table 1)
(Connon *et al.* 2014; Haynes *et al.* 2018). Given that this period of discharge monitoring
350 coincided with a period of considerable climate warming and documented land cover change at
Scotty Creek, the trend in calculated runoff over the period of record reflects a shift from a
permafrost plateau-dominated landscape to one increasingly influenced by hydrologically-
connected wetlands. Therefore, the temporal trend of runoff from the Scotty Creek basin is
driven by permafrost thaw-induced land cover change (Connon *et al.* 2014; Haynes *et al.* 2018).

355

Table 1: Annual precipitation (2008-2019), basin runoff (1996-2015; Connon *et al.* 2014; Haynes *et al.* 2018), evapotranspiration (2013-2016; Warren *et al.* 2018), and residual storage values are presented (mm year⁻¹) for two distinct transitional landscape stages at Scotty Creek: a landscape dominated by forest and a patchwork landscape of near-equal forest and treeless wetland land covers.

360

	FOREST > WETLAND	FOREST ≈ WETLAND
PRECIPITATION	493	493
RUNOFF	149	215
EVAPOTRANSPIRATION	206	255
RESIDUAL STORAGE	138	23

365

370

Recent work by Warren *et al.* (2018) examined evapotranspiration (ET) for forests, wetlands, and the integrated landscape within the Scotty Creek watershed between 2013 and 2016. Daily ET values (mm day⁻¹) reported by Warren *et al.* (2018) were converted to annual ET (mm year⁻¹) for the purpose of the conceptual framework water balance in the present work (Table 1). The different land covers monitored by Warren *et al.* (2018) are representative of the land cover end-members identified in our conceptual framework. Therefore, the annual ET values based on the data collected by Warren *et al.* (2018) for the black spruce forests, open collapse scar wetlands and the integrated landscape were associated with the appropriate stage along our proposed trajectory of change. Stages of the trajectory for which representative measurements were not collected are interpolated between the land cover end-members for which ET was measured.

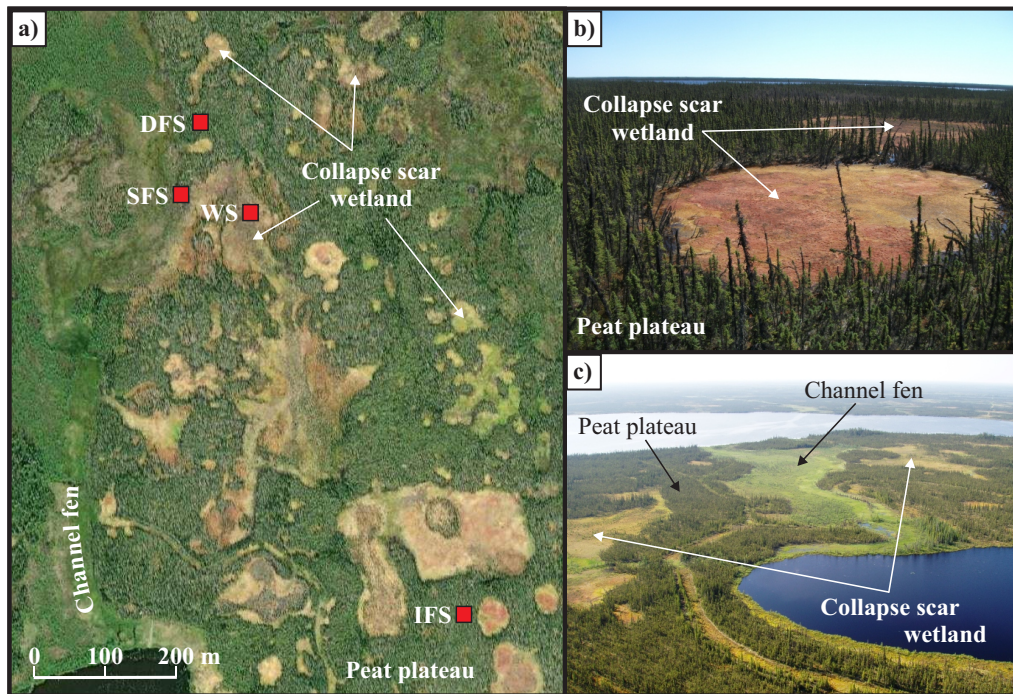
375

Given the insignificant changes in annual precipitation over the period of measurement (Connon *et al.* 2014; Haynes *et al.* 2018), annual storage was calculated as the residual of annual precipitation inputs, and annual evapotranspiration and runoff outputs for the conceptual framework water balance (Table 1).

3.4 Radiation Fluxes

Four meteorological stations at Scotty Creek were selected for use in this study (Figure 3). This included a station installed in a collapse scar wetland in 2004 (hereafter “wetland station”) followed by a second station on a densely forested peat plateau in 2007 (hereafter “dense forest station”). The radiation flux data from these two stations are representative of the collapse scar wetland and permafrost plateau land cover types, respectively. Two additional stations located on forested plateaus were also used to represent tree canopy densities different from that of the dense forest station. These stations were installed on a sparsely forested peat plateau in 2015 (hereafter “sparse forest station”) and a forested plateau with a canopy of intermediate density between that of the dense and sparse stations in 2014 (hereafter “intermediate forest station”). All radiation measurements were made below the tree canopy at a height of 2 m above the ground surface. Four component radiation data were collected at the dense forest, sparse forest, and wetland meteorological stations, while only shortwave radiation was collected at the intermediate forest station. The reader is directed to Haynes *et al.* (2019) for full descriptions of the radiation instrumentation within the Scotty Creek basin. Radiation was measured every minute, and averaged and recorded every 30 minutes from which daily (24 hourly) averages were computed. The daily averages were then used to compute annual average radiation for each station. While these computations defined some of the variability of radiation fluxes among land cover types, they do not account for flux variations over short temporal and spatial scales (Webster *et al.* 2016). To address these, the daily average four component radiation data from each station were compared on a monthly time step. The monthly averages were calculated and compared across the land covers represented by each of the four meteorological stations using a one-way analysis of variance (ANOVA) with Tukey post-hoc test ($\alpha = 0.05$),

400 thereby testing the effect of land cover on monthly shortwave and longwave incoming and outgoing radiation.



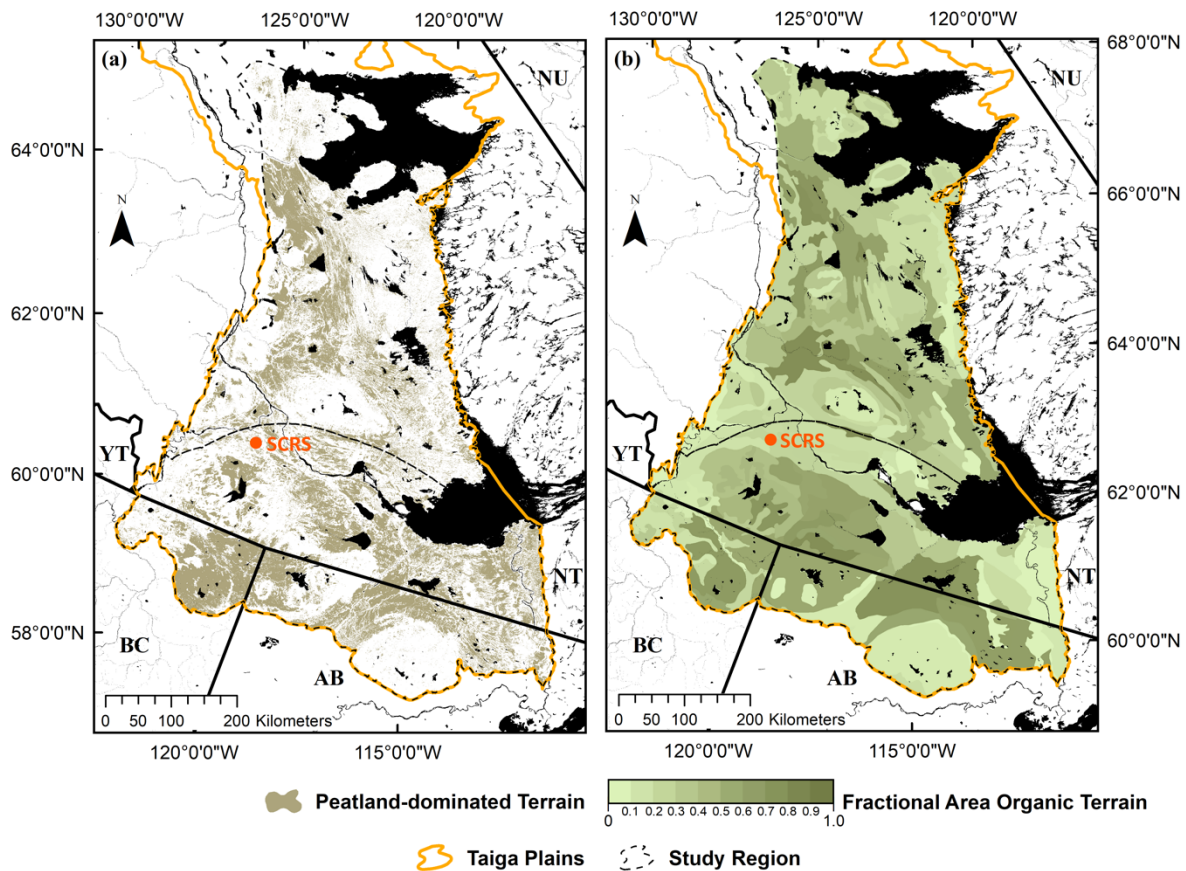
405 Figure 3: Worldview 2 satellite image (a) and oblique aerial photographs (b, c) over Scotty Creek, Northwest Territories. The satellite image also shows the locations of the Dense Forest Station (DFS), Sparse Forest Station (SFS), Wetland Station (WS) and Intermediate Forest Station (IFS) micrometeorological stations. The oblique aerial photographs show the land cover types that dominate lowlands with discontinuous permafrost in the Taiga Plains including peat plateau (permafrost), collapse scar wetland, and channel fen.

410 4. Results and Discussion

4.1 Peatland and Forest Occurrence

The type of peatland-dominated terrain composed of peat plateau-wetland complexes separated by channel fens as described for Scotty Creek, occupy approximately 35% of the discontinuous permafrost zones of the Taiga Plains (Figure 4a). Large peatland clusters are
415 located in lowland areas with high histel or histosol soil percentages. In the extensive-discontinuous permafrost zone, peatlands are clustered to the west near to the Mackenzie River,

and are largely absent from the eastern portion of the study area in the region bounded by Great Bear Lake to the north and the Taiga Shield to the east. In the sporadic-discontinuous zone however, the peatland clusters are more longitudinally dispersed.



420

Figure 4: Predicted distribution of peatland-dominated terrain in the discontinuous permafrost zone of the Taiga Plains (a). Peatland-dominated terrain was mapped using a saturated soils dataset (Natural Resources Canada 2017) (a) and compared to the NCSCD (Bolin Centre for Climate Research 2013) (b). Contains information licensed under the Open Government Licence – Canada.

425

Comparing the fractional areas of probable peatland terrain from the saturated soils dataset to the NCSCD showed the saturated soils dataset was more likely to overstate the distribution of probable peatland terrain compared to the NCSCD maps. Approximately 20% of the fractional areas were exact matches between the two datasets, 20% were lower in the

430

saturated soils dataset, and 60% were higher in the saturated soils dataset. However, despite these disagreements, 79% of the fractional areas determined using the saturated soils dataset were within 15% of the fractional areas in the NCSCD. This suggests that using the Natural Resources Canada saturated soils dataset may be an appropriate method of mapping probable
435 peatland terrain in the Taiga Plains on a finer scale (Figure 4a) compared to the broad zones presented by the NCSCD (Figure 4b). Only 11 of the 572 NCSCD zones (~2%) had disagreements over 25% when comparing the fractional areas between both datasets. The majority of these zones of disagreement were located along the Slave River, in the far southeast of the Taiga Plains study region.

440 A latitudinal trend in land cover percentage was found for the mapped peatland-dominated terrain (Figure 5). Along the boundary between the extensive-discontinuous and sporadic-discontinuous permafrost zones near the centre of the study region, collapse scar wetland features are most prevalent. Median fractional forest cover in peatlands (*i.e.* peat plateaus or treed wetlands) reaches its minimum value of 33% within the 61° N bin, near the
445 latitude of Scotty Creek. The proportion of forested peatlands remains relatively low throughout the transitional zone between sporadic and extensive discontinuous permafrost (approximately 61° to 62° N) where the median forest cover does not exceed 34%. The widespread occurrence of collapse scars suggest that permafrost thaw and the resulting processes of ground surface subsidence and inundation are particularly active in this zone compared to the extensive
450 discontinuous permafrost zone to the north and the sporadic discontinuous permafrost zone to the south, where the fractional forested areas are higher.

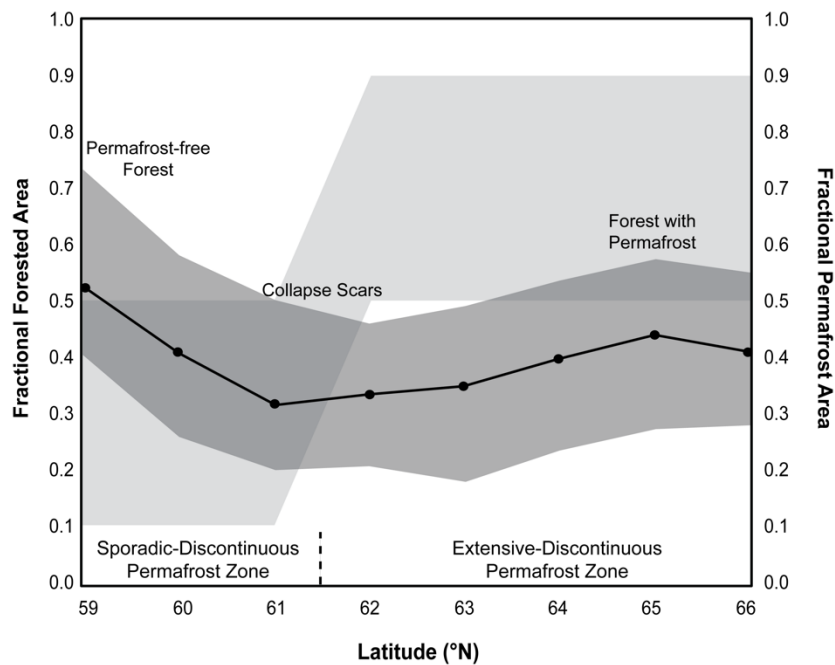


Figure 5: Median forested peatland area expressed as a fraction of the total peatland area and plotted as a function of latitude. The dark grey area represents the range in the proportion of the landscape occupied by forested peatland (i.e. fractional forested area) between the 25th percentile and 75th percentile. The lighter grey area indicates the range in the proportion of landscape underlain by permafrost (i.e. fractional permafrost area) as indicated by Brown *et al.* (2002).

455

460

The median proportion of forested peatlands in the extensive-discontinuous zone (63° to 66° N) ranges from approximately 35 to 45%, indicating that permafrost thaw is less prevalent over the landscape than in the transition zone immediately to the south. However, the median fractional forested area is at its greatest (52%) south of the transition in the sporadic-discontinuous zone (59° to 60° N), where about half of the peatland area is forest covered.

465

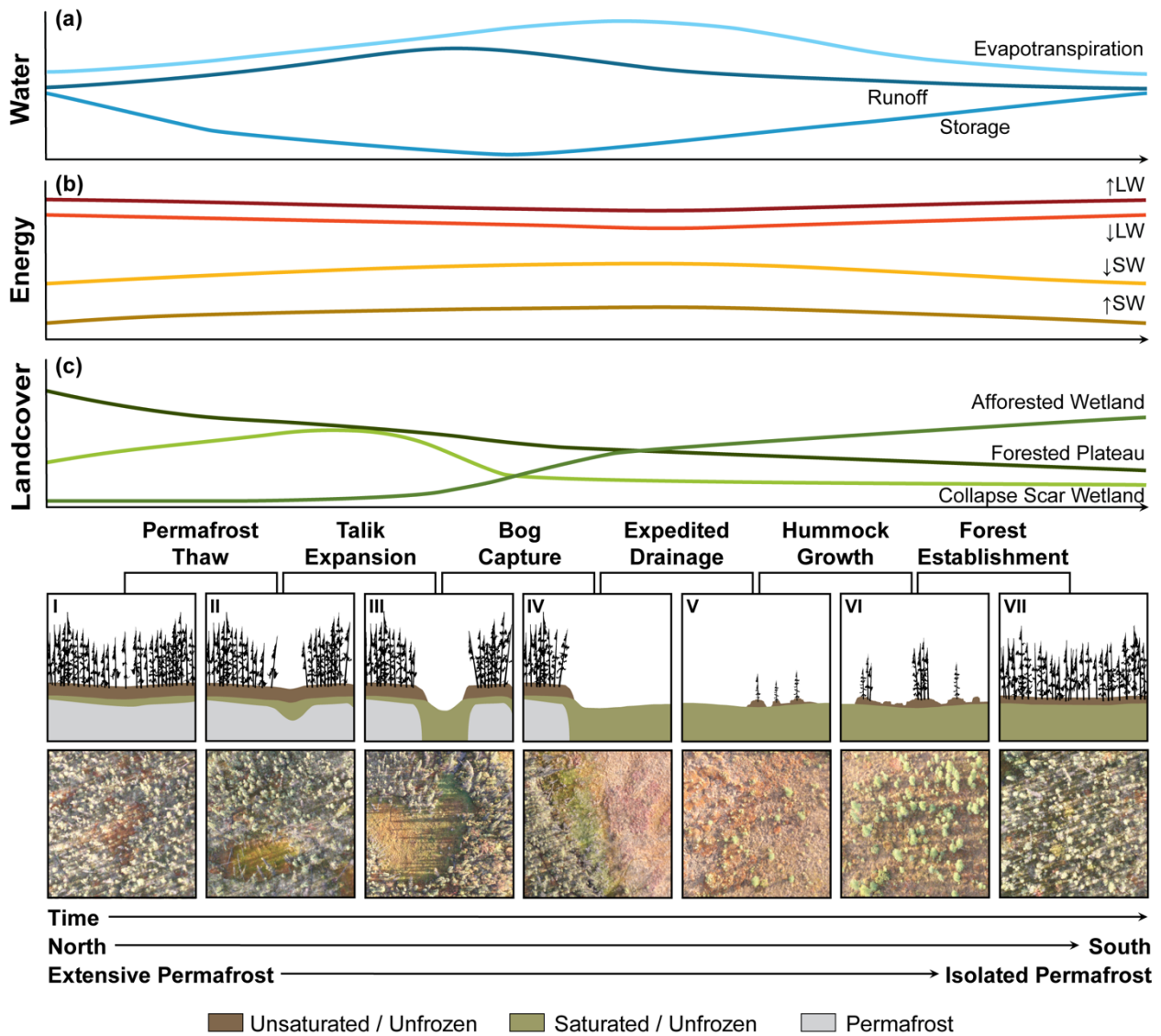
Expansion of forest cover in this zone, especially in the areas of north-eastern British Columbia and north-western Alberta, has been reported by others (*e.g.* Zoltai 1993, Carpino *et al.*, 2018). A pattern of forest expansion over permafrost-free terrain is consistent with the observation of a northward-moving southern limit of permafrost reported by Kwong and Gan (1994) and with the process of tree re-establishment following permafrost thaw-induced partial drainage of wetlands

470

described by Haynes *et al.* (2020).

4.2 Conceptual Framework of Land Cover Change

From the remote sensing and field-based hydrological studies at Scotty Creek since the mid-1990s, key insights into incremental land cover changes initiated by permafrost thaw have emerged. Using this knowledge as a foundation, the present study examines both the hydrological and radiation regimes of each incremental stage and the land cover changes over the larger region in which permafrost thaw is known to be widely occurring and within which the southern edge of permafrost is migrating northward (Kwong & Gan, 1994). From this approach, a new conceptual framework is presented (Figure 6), which describes permafrost thaw-induced land cover change in the peatland-dominated regions of the discontinuous permafrost zone. The land cover change occurring simultaneously (to varying degrees) at Scotty Creek and latitudinally across the wider Taiga Plains region can be categorized into seven distinct land cover stages, the first and last of which are forest cover, with the difference being that the former overlies permafrost and the latter does not. The stages are as follows: (I) Forested permafrost plateaus; (II) Forested permafrost plateaus with small, isolated collapse scars; (III) Forested permafrost plateaus with larger, interconnected wetlands; (IV) Wetland complexes with small plateau islands; (V) Wetland complexes with hummock development and tree establishment; (VI) Hummock growth with forest establishment; and (VII) Forested peatlands (Figure 6). In the following sections, the biophysical, hydrological and radiation regimes of each of these stages are presented and discussed, drawing on several investigations in the region.



490

495

500

Figure 6: (Bottom) Proposed conceptual framework of landscape trajectory including a space-for-time substitution for changes to both permafrost and land cover. Conceptual diagrams are presented to illustrate landscape change with the support of RPAS imagery collected in the Scotty Creek basin. The conceptual framework is presented alongside the processes that initiate the trajectory's progression. (a) Relative changes to local water balances of measured Scotty Creek basin runoff, evapotranspiration and residual storage with unchanging precipitation are summarized and presented over the trajectory of landscape change based on the proportion of forested vs. wetland area. (b) Relative changes to local energy balances are presented using data collected from sub-canopy meteorological stations installed at Scotty Creek. (c) Changes to relative land cover proportions are presented using historical aerial photographs and recent acquisitions of satellite imagery over the Scotty Creek basin.

4.2.1 Biophysical Characteristics

505 The present study found that the early land cover stages presented in Figure 6 are more prevalent at the higher latitudes of the study region and the later stages at the lower latitudes. Considering that permafrost thaw is more advanced in the lower latitudes and that the southern limit of permafrost is advancing northward (Kwong & Gan, 1994), it is reasonable to expect that the more advanced stages presently characterising the lower latitudes will, in the future, 510 characterise the higher latitudes, assuming a continuation of climate warming induced permafrost thaw. Approaching a change in latitude through the study region as analogous to a change in land cover stage, or more specifically, to a change in time, is supported by studies that examined land cover change over the last half-century at Scotty Creek (Chasmer & Hopkinson, 2017; Quinton *et al.*, 2019) and along a north to south transect extending from Scotty Creek to northeastern 515 British Columbia (Carpino *et al.*, 2018).

 The Scotty Creek basin, located near the northern limit of sporadic discontinuous permafrost (Figure 1) is characterised mainly by stages III and IV. However, examples of all seven stages can be found in local areas at Scotty Creek. For this reason, the long term monitoring and research programs at Scotty Creek involving each of these land cover types 520 contributes detailed information on their form and functioning, and on their transition from one to another. For example, permafrost thaw changes a landscape dominated by forested plateaus (Figure 6I) to one with small, suprapermafrost taliks (Connon *et al.* 2018) and isolated collapse scars (Figure 6II; Quinton *et al.* 2011). Continued thaw expands isolated collapse scars (Figure 6III; Devoie *et al.* 2019) enabling them to coalesce to form interconnected wetlands (Connon *et al.* 2015), a process that then leads to a landscape of expansive wetlands dotted with isolated 525 plateau “islands” (Figure 6IV; Baltzer *et al.* 2014; Chasmer & Hopkinson 2017). Since the process of wetland expansion removes peat plateaus, a land cover type that impounds wetlands

and obstructs drainage (Connon *et al.*, 2014), this process enables the landscape drain more efficiently (Haynes *et al.*, 2018). As wetlands drain, hummock micro-topography develops in their relatively drier interiors (Figure 6V; Haynes *et al.* 2020), which allows black spruce to colonise the wetlands on the relatively dry hummock surfaces (Figure 6VI; Iversen *et al.* 2018; Dymond *et al.* 2019). Continued drainage and drying of wetlands enables the expansion of their hummocky terrain and therefore of their tree cover (Eppinga *et al.* 2007; Iversen *et al.* 2018) until the landscape returns to a more continuous forest cover (Figure 6VII; Carpino *et al.* 2018). However, the forest cover in this final stage is permafrost-free and for that reason, the conceptual framework presented in Figure 6 stands in contrast to those presented by Zoltai (1993) and Camill (1999) in which the re-emergence of a forest cover relies on the re-emergence of the underlying permafrost. According to Zoltai (1993), forest re-emerges because permafrost displaces the overlying ground surface upward, resulting in the development of an unsaturated layer suitable for tree establishment. By contrast, the tree establishment described in Figure 6 results not from the re-emergence of permafrost, but from its continued thaw over the landscape, a process that dewateres wetlands (Connon *et al.*, 2014; Haynes *et al.*, 2018) to the extent suitable for tree establishment (Haynes *et al.* 2020).

The concept of land cover transition depicted in Figure 6 also stands in contrast to those that couple forest with permafrost thaw and re-development in terms of the time frame. Permafrost-enabled re-establishment of forest requires a minimum of several centuries to complete (Zoltai, 1993; Treat & Jones, 2018) whereas the wetland drainage enabled re-establishment of forest (Figure 6) occurs in less than half a century as suggested by the archived imagery for Scotty Creek. There, the early stages (*i.e.* stages I, II) represent the changes observed between 1947 and 2000 over which time the tree-covered area decreased from approximately 70% to approximately 50% (Quinton *et al.* 2011). The fraction of forested land above

permafrost-free terrain cover is unknown for this period but assumed to be negligible based on land cover descriptions for this region (e.g. NWWG, 1988; Zoltai 1993; Robinson & Moore, 2000). This period therefore generated a concomitant rise in the cover of wetlands over the
555 landscape (*i.e.* 30 to 50%) since permafrost thaw transitions the tree covered plateaus to collapse scars and channel fens, as confirmed by analysis of archived imagery (Chasmer *et al.*, 2010). By 2018, tree-covered peat plateaus decreased to 40%, and treeless wetlands occupied 45% of the land cover (13% collapse scars and 32% channel fens) (Disher 2020). These studies indicate that permafrost thaw and the resulting processes have both removed forest as a result of thaw-induced
560 subsidence and inundation of plateau surfaces, and more recently, enabled forest re-establishment in the form of treed wetlands (Haynes *et al.* 2020; Disher *et al.*, 2021). However, the dominant land cover transition at Scotty Creek is still from forest (peat plateau) to wetland as a result of permafrost thaw, resulting in a net forest loss, a process that will continue until the later stages of Figure 6 are reached (*i.e.* stages VI, VII), at which point there will be a net forest
565 gain.

The sequence of land cover stages following permafrost thaw observed at Scotty Creek and depicted in Figure 6 is supported by vegetation successional changes described in the literature for wetlands as they age. For example, aquatic *Sphagnum* species, notably *S. riparium*, are the first to occupy the inundated margins between thawing permafrost plateaus and
570 developing collapse scars (Garon-Labrecque *et al.* 2015; Pelletier *et al.* 2017). Such recent areas of collapse are easily identified on high-resolution RPAS imagery by the distinct bright green colour of *S. riparium* (Figure 6II, III, IV; Gibson *et al.* 2018; Haynes *et al.* 2020). These wetland-plateau edges may also be identified by bare peat or moats of water (Zoltai 1993). As collapse scars expand, lawn species, such as *S. angustifolium*, and hummock species, such as *S.*
575 *fuscum*, emerge, particularly in the drier interior of wetlands (Zoltai 1993; Camill 1999; Pelletier

et al. 2017). Hummock species, mainly *S. fuscum*, first emerge near the centre of collapse scars, and expand outward over time (Camill 1999; Loisel & Yu 2013). Much like *S. riparium*, *S. fuscum* is also easily identified in high-resolution imagery, where *S. fuscum* is distinguished by its russet colour (Figure 6V) (Haynes *et al.* 2020). As the density of the *S. fuscum* hummocks increases, imagery and ground-based observations indicate the presence of young black spruce trees (Liefers & Rothwell 1987; Haynes *et al.* 2020), first on isolated hummocks (Figure 6VI) but eventually as widespread afforestation (Figure 6VII; Camill 2000; Ketteridge *et al.* 2013).

4.2.2 Radiation Flux Characteristics

The Scotty Creek basin is a microcosm of its larger regional setting since it contains each of the land cover stages of the conceptual framework in Figure 6. As such, the micro-meteorological measurements made at Scotty Creek for different land cover types provide insight into how energy regimes change as one land cover stage transitions to the next. Both incoming and outgoing shortwave radiation peak at the middle stages (IV, V), where treeless collapse scars predominate. Annual incoming and outgoing shortwave radiation is lowest at the dense forest station, which represents the initial stage (I). Likewise, incoming and outgoing annual longwave radiation are greatest in the early (I, II) and late stages (VI, VII) and lowest in the wetland-dominated middle stages (IV, V).

Statistically significant differences were found between stations for incoming (Figure 7a) and outgoing (Figure 7b) shortwave and incoming longwave radiation (Figure 7c), while there was no statistical differences between stations for outgoing longwave (Figure 7d). However, Tukey post-hoc tests revealed variability between the two shortwave components in terms of which groups showed these significant differences. As the four meteorological stations fall along a gradient of forest density from treeless wetland to a densely forested plateau, no significant

differences in incoming shortwave radiation were ever found between stations only one rank
600 apart on that gradient. As such, measurements indicate average monthly incoming shortwave
radiation is significantly greater at the wetland compared to both the intermediate forest ($p <$
0.05) and the dense forest ($p < 0.05$), while no significant difference exists between wetland and
the sparse forest. However, the dense forest receives significantly less incoming shortwave
radiation than both the wetland ($p < 0.05$) and the sparse forest ($p < 0.05$), but this station is not
605 significantly different from the intermediate forest.

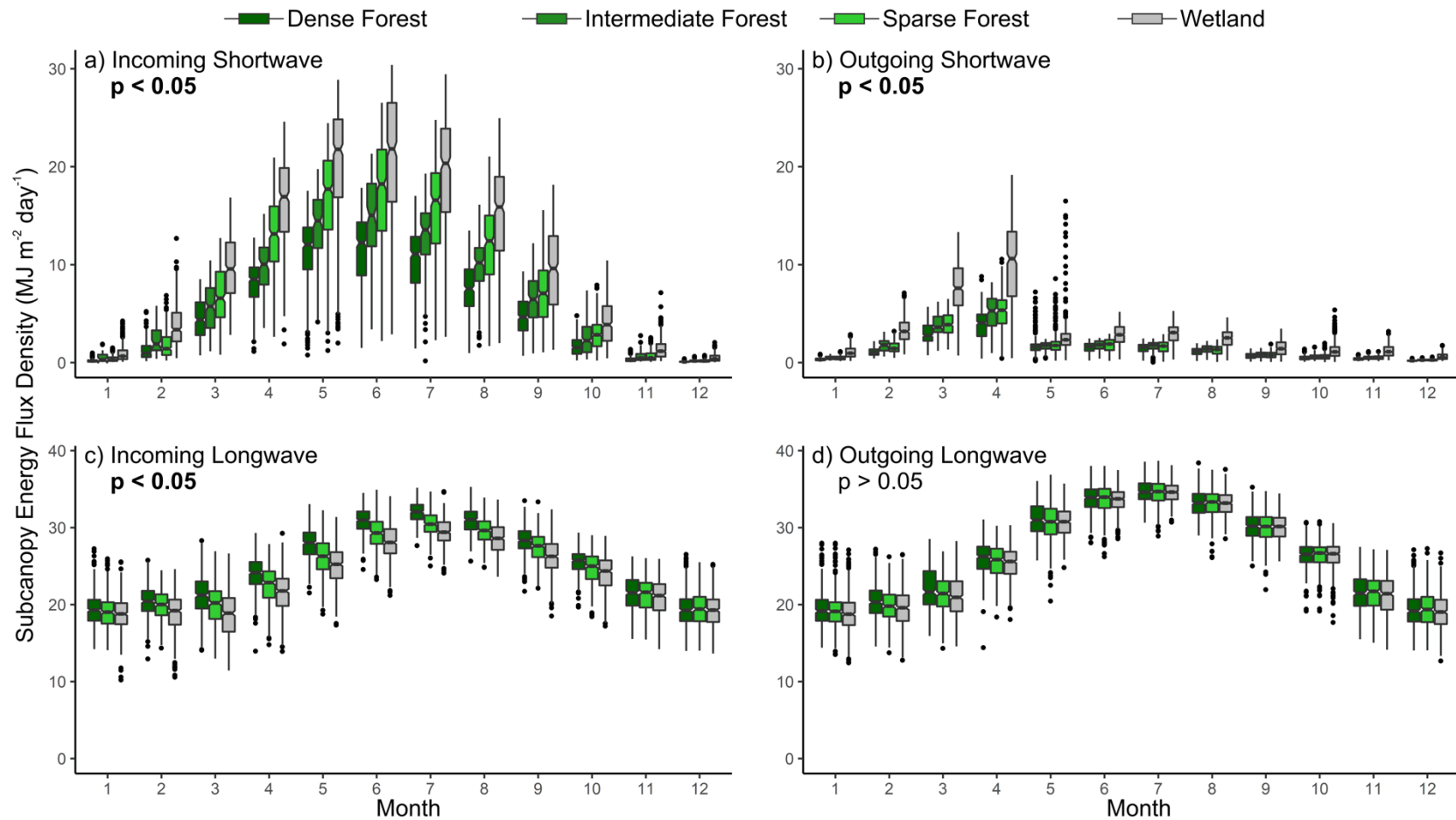
No significant differences in outgoing shortwave radiation exist between any of the
forested plateau stations but all are significantly different from the wetland. Specifically,
outgoing shortwave radiation recorded at the wetland station is significantly greater than the
sparse forest ($p < 0.05$), intermediate forest ($p < 0.05$), and dense forest stations ($p < 0.05$). The
610 differences between the wetland station and the forested plateau stations are also increasingly
significant with increasing tree density. There was a statistically significant difference between
the three stations (intermediate forest omitted due to lack of measurements) for incoming
longwave radiation, while no statistically significant differences were observed in the outgoing
longwave radiation component. The only significant difference in incoming longwave was
615 observed between the wetland and dense forest ($p < 0.05$). No significant differences exist
between the sparse forest and the wetland or dense forest.

The comparison among the plateau stations of contrasting tree canopy densities provides
insight into the permafrost thaw-induced progression of radiation regimes as plateaus transition
to wetlands, a process involving the gradual thinning and eventual loss of the tree canopy.
620 Wright *et al.* (2009) demonstrated that small-scale changes to the tree canopy density can
increase insolation to the ground in localized areas leading to thaw depressions in the active layer

and water flows toward such depressions from their surroundings. Such areas of preferential thaw therefore develop elevated soil moisture contents, and since soil thermal conductivity increases with its moisture content, the preferential thaw process is reinforced. This is suggested
625 as the mechanism driving the transition from stage I to II in the trajectory (Quinton *et al.* 2019). This feedback is present in the initial stages of the trajectory, and is often associated with talik formation and expansion into collapse scars due to localized permafrost loss (Chasmer & Hopkinson 2017; Connon *et al.* 2018). Such thaw can extend to the base of the active layer in which case further thaw results in permafrost loss, ground surface subsidence, waterlogging of
630 the ground surface, local tree mortality, and therefore further thinning of the overlying tree canopy and consequently more insolation at the ground surface. These processes and feedback mechanisms are critical in the generation of collapse scars in stage III.

Differing ground surface properties, particularly albedo, can amplify the differences in incoming shortwave radiation among the land covers. However, the difference in mean albedo
635 during the snow-free season (May-September) below the plateau canopies is less than 5% and displays a small increasing gradient as the canopy becomes more dense (sparse: 0.111, intermediate: 0.127, dense: 0.147). The mean wetland albedo (0.145) during the snow-free season is also similar to the plateau surfaces and most closely resembles the surface albedo of the dense plateau. The greatest contrast in albedo occurs during the period of several weeks while
640 snow still covers the plateaus but is absent on the adjacent wetlands (Connon *et al.*, *Submitted*). This contrast in albedo is also evident in Figure 7b, which shows that following winter, outgoing shortwave radiation from the wetland increases before the forested stations. Helbig *et al.* (2016b) attributed their observed increase in landscape albedo in this late winter/spring period to the permafrost thaw-induced conversion of forest (lower albedo) to wetland (higher albedo), and
645 suggested that this could lead to a regional cooling effect during this time of the year. However,

that study implicitly assumed that the wetlands were a final land cover stage rather than an incremental step toward the re-establishment of forest as depicted in the conceptual framework presented in Figure 6.



650 Figure 7: Sub-canopy daily total (MJ/m²/day) incoming shortwave (a), outgoing shortwave (b), incoming longwave (c), and
 655 outgoing longwave (d) at the four meteorological stations. Each station represents a distinct land cover: dense forest (2007-2019),
 intermediate forest (2014-2019), sparse forest (2015-2018), and treeless wetland (2004-2019). The boxes represent the 25th and
 75th percentile, while the whiskers represent the range of the data. The notches on each box indicate the confidence interval ($\alpha =$
 0.05) around the mean while the statistical differences between meteorological stations have been presented in the upper left of
 each plot as determined by one-way ANOVA. Significant p values have been highlighted with bold text.

4.2.3 Hydrological Characteristics

As the land covers presented in the conceptual framework transition from one to the next, hydrological processes also change (Figure 6a). In the early stages (I, II), a relatively large proportion of hydrological inputs from the atmosphere are stored in collapse scars due to their impoundment by the permafrost on their margins (Connon *et al.* 2014). Evapotranspiration from the landscape is relatively low given the high proportion of forest and relatively low transpiration by the black spruce that dominates the plateau canopies (Warren *et al.* 2018). In the early land cover stages (I, II) when forests predominate, understory vegetation provide the pathway for evapotranspiration (Chasmer *et al.* 2011). The incremental change in land covers presented in Figure 6 involves biophysical changes that affect the partitioning of precipitation into storage or runoff. By stage III to IV wetlands are interconnected and rapidly expanding, the storage of water on the landscape reaches its minimum level while runoff from the landscape is maximized (Figure 6a). This increased runoff is enabled by the removal of permafrost barriers (Haynes *et al.* 2018) and areal expansion of runoff contributing areas resulting in greater hydrological connectivity and therefore drainage of the landscape (Connon *et al.* 2014). These observations coincide with a period of steady, unchanging annual precipitation; therefore precipitation does not account for elevated basin runoff (Connon *et al.* 2014). A decrease in landscape drainage then follows in the subsequent stages as the transient runoff contributions from “captured” collapse scars diminishes as the importance of evapotranspiration increases as the wetlands become the predominant land cover (IV, V). The increase in evapotranspiration is due to increases in evaporation from areas occupied by standing water and saturated or near-saturated wetland vegetation, including *Sphagnum* mosses, with losses due to transpiration driven by shrub vegetation (Warren *et al.* 2018). In the advanced stages (VI, VII) evapotranspiration would decrease as a result of the drier wetland surfaces as hummock microtopography replaces

680 saturated *Sphagnum* lawns. The treed (afforested) wetlands (VII) have not been studied to the same degree as peat plateaus or collapse scar wetlands (Haynes *et al.* 2020; Disher *et al.*, 2021) and therefore ground based hydrological data specific to these features are lacking.

5. Conclusions

The discontinuous permafrost zone of the Taiga Plains exemplifies a landscape in transition. Coupling a broad-scale mapping initiative with the detail of site-specific data collected in the Scotty Creek basin demonstrates a permafrost thaw-induced land cover transition. This transition is incremental and involves distinct land cover stages. The first and last of these is a continuous forest cover, although in the first stage the forest is underlain by permafrost while in the last stage it is not. Unlike traditional concepts of land cover change in peatland dominated regions of discontinuous permafrost in which forest re-establishment occurs over centuries and is constrained by the rate of permafrost re-development, the concept presented here described forest re-establishment within decades and resulting from continued permafrost thaw, a process which allows wetlands to de-water sufficiently for tree growth. Each land cover stage has characteristic biophysical, hydrological and micro-meteorological features.

695 The proposed conceptual framework of landscape evolution describes the transitions occurring across the Taiga Plains in peat plateau-collapse scar wetland complexes like Scotty Creek. This study also identifies the applicability of this conceptual framework across a large region of the Canadian north. We establish the likely pattern of change across these peat plateau-collapse scar wetland complexes and project their future trajectory by combining long-term field observations with analyses of contemporary and historical imagery. It is proposed that, while permafrost thaw-induced land cover changes have previously been dominated by a transition from forest to wetland, this transition is not permanent and forested land covers are likely to

return over time, although unlikely to be underlain by permafrost. This research improves the understanding of how peat plateau-collapse scar wetland complexes in the Taiga Plains may be impacted by ongoing permafrost thaw and these results may also be of relevance to other peatland-rich permafrost environments across the circumpolar north.

6. Acknowledgements

We gratefully acknowledge the support of the Dehcho First Nations, in particular, the Liidlii Kue First Nation and Jean Marie River First Nation. We also thank these communities for their long-standing support of the Scotty Creek Research Station. This work was funded by ArcticNet through their support of the Dehcho Collaborative on Permafrost (DCoP), and by the Natural Sciences and Engineering Research Council of Canada (NSERC). We also acknowledge the Canada Foundation for Innovation (CFI) for providing funding for infrastructure critical to this study.

7. Data Availability

The radiation flux data used in this paper are catalogued for open access in the Wilfrid Laurier University (WLU) Data Repository at <https://doi.org/10.5683/SP2/JTIQDO>.

8. Author Contributions

All authors contributed to the development of the research question and the methodological approach used in this study. OC and RC performed the analyses. OC, KH, and WQ wrote the manuscript with input and editorial contributions from RC, JC, and ÉD.

9. Competing Interests

The authors declare that they have no conflict of interest.

10. References

- 725 Baltzer, J., Veness, T., Chasmer, L., Sniderhan, A., & Quinton, W. (2014). Forests on thawing permafrost: Fragmentation, edge effects, and net forest loss. *Global Change Biology*, 20(3), 824-834. DOI: 10.1111/gcb.12349
- Beilman D.W. & Robinson S.D. (2003). Peatland permafrost thaw and landcover type along a climate gradient. Proceedings of the Eighth International Conference on Permafrost, vol. 730 1. Phillips M., Springman S.M., & Arenson L.U., Eds. Balkema, Zurich, pp 61–65.
- Biskaborn, B.K., Smith, S.L., Noetzi, J. *et al.* (2019). Permafrost is warming at a global scale. *Nature Communications*, 10(264). doi.org/10.1038/s41467-018-08240-4
- Bolin Centre for Climate Research (2013). The Northern Circumpolar Soil Carbon Database. Available at: <https://bolin.su.se/data/nscsd/> (Accessed March 20, 2019)
- 735 Box, J.E., Colgan, W.T., Christensen, T.R., Schmidt, N.M., Lund, M., Parmentier, F.W., Brown, R., Bhatt, U.S., Euskirchen, E.S., Romanovsky, V.E., Walsh, J.E., Overland, J.E., Wang, M., Corell, R.W., Meier, W.N., Wouters, B., Mernild, S., Mård, J., Pawlak, J. & Olsen, M.S. (2019). Key indicators of arctic climate change: 1971-2017. *Environmental Research Letters*, 14, 045010. doi.org/10.1088/1748-9326/aafc1b
- 740 Brown, R. J. E.: 1964, Permafrost Investigations on the Mackenzie Highway in Alberta and Mackenzie District, Technical Paper No. 175, Division of Building Research, National Research Council, Canada.
- Brown, J., O. Ferrians, J. A. Heginbottom, and E. Melnikov. (2002). Circum-Arctic Map of Permafrost and Ground-Ice Conditions, Version 2. Permaice subset used. Boulder, 745 Colorado USA. NSIDC: National Snow and Ice Data Center. Date accessed: Jan. 2020.
- Camill, P. (1999). Peat accumulation and succession following permafrost thaw in the boreal peatlands of Manitoba, Canada. *Ecoscience*, 6(4), 592-602.
- Camill, P. (2000). How much do local factors matter for predicting transient ecosystem dynamics? Suggestions from permafrost formation in boreal peatlands. *Global Change* 750 *Biology*, 6, 169-182. doi.org/10.1046/j.1365-2486.2000.00293.x
- Camill, P. & J. S. Clark, 1998. Climate change disequilibrium of boreal permafrost peatlands caused by local processes. *American Naturalist*, 151, 207-222. DOI: 10.1086/286112
- 755 Carpino, O.A., Berg, A.A., Quinton, W.L., & Adams, J.R. (2018). Climate change and permafrost thaw-induced boreal forest loss in northwestern Canada. *Environmental Research Letters*, 13(8). doi.org/10.1088/1748-9326/aad74e
- Chasmer, L. & Hopkinson, C. (2017). Threshold loss of discontinuous permafrost and landscape evolution. *Global Change Biology*, 23, 2672-2686.
- Chasmer, L., Hopkinson, C. & Quinton, W. (2010). Quantifying errors in discontinuous permafrost plateau change from optical data, Northwest Territories, Canada: 1947-2008. 760 *Canadian Journal of Remote Sensing*, 36(2), 211-223. DOI: 10.1111/gcb.13537
- Chasmer, L., Hopkinson, C., Veness, T., Quinton, W., & Baltzer, J. (2014). A decision-tree classification for low-lying complex landcover types within the zone of discontinuous

permafrost, *Remote Sensing of Environment*, 143, 73–84.
doi.org/10.1016/j.rse.2013.12.016

- 765 Chasmer, L., Quinton, W., Hopkinson, C., Petrone, R., & Whittington, P. (2011). Vegetation Canopy and Radiation Controls on Permafrost Plateau Evolution within the Discontinuous Permafrost Zone, Northwest Territories, Canada. *Permafrost and Periglacial Processes*, 22(3). doi.org/10.1002/ppp.724
- 770 Cohen, J., Screen, J. A., Furtado, J. C., Barlow, M., Whittleston, D., Coumou, D., Francis, J., Dethloff, K., Entekhabi, D., Overland, J., & Jones, J. (2014). Recent Arctic amplification and extreme mid-latitude weather, *Nature Geoscience*. doi.org/10.1038/ngeo2234
- Connon, R., Devoie, É., Hayashi, M., Veness, T., & Quinton, W. (2018). The influence of shallow taliks on permafrost thaw and active layer dynamics in subarctic Canada. *Journal of Geophysical Research: Earth Surface*, 123, 281–297. doi.org/10.1002/2017JF004469
- 775 Connon, R.F., Quinton, W.L., Craig, J.R., & Hayashi, M. (2014) Changing hydrologic connectivity due to permafrost thaw in the lower Liard River valley, NWT, Canada *Hydrol Process.*, 28, 4163–78. doi.org/10.1002/hyp.10206
- Connon, R. F., Quinton, W.L., Craig, J.R., Hanisch, J., & Sonnentag, O. (2015). The hydrology of interconnected bog complexes in discontinuous permafrost terrains *Hydrol. Process.* 29, 3831-47. doi.org/10.1002/hyp.10604
- 780 Connon, R., Chasmer, L., Helbig, M., Hopkinson, C., Sonnentag, O., Quinton, W., & Haughness, E. (Submitted 2021). The implications of permafrost thaw and landcover change on snow water equivalent accumulation, melt and runoff in discontinuous permafrost peatlands. *Hydrologic Processes*
- 785 DeAngelis, A., Qu, X., Zelinka, M., & Hall, A. (2015). An observational radiative constraint on hydrologic cycle intensification. *Nature*, 528, 249-253. DOI: 10.1038/nature15770
- Devoie, É.G., Craig, J.R., Connon, R.F., & Quinton, W.L. (2019). Taliks: A tipping point in discontinuous permafrost degradation in peatlands. *Water Resources Research*, 55(11), 9838-9857. doi.org/10.1029/2018WR024488
- 790 Disher BS, Connon RF, Haynes KM, Hopkinson C, Quinton WL. (2021). The hydrology of treed wetlands in thawing discontinuous permafrost regions. *Ecohydrology*, doi.org/10.1002/eco.2296.
- Disher, B.S. (2020). Characterising the hydrological function of treed bogs in the zone of discontinuous permafrost, M.Sc. Thesis, Wilfrid Laurier University, Waterloo, 72 pp.
- 795 Dymond, S.F., D'Amato, A.W., Kolka, R.K., Bolstad, P.V., Sebestyen, S.D., Gill, K., & Curzon, M.T. (2019). Climatic controls on peatland black spruce growth in relation to water table variation and precipitation. *Ecohydrology*, 2137. doi.org/10.1002/eco.2137
- Environment and Climate Change Canada. Adjusted and homogenized Canadian climate data. Available at: <https://www.canada.ca/en/environment-climate-change/services/climate-change/science-research-data/climate-trends-variability/adjusted-homogenized-canadian-data.html> (Accessed June 1, 2020)
- 800

- Eppinga, M.B., Rietkerk, M., Wassen, M.J., & De Ruiter, P.C. (2007). Linking habitat modification to catastrophic shifts and vegetation patterns in bogs. *Plant Ecol.* 200, 53-68. doi.org/10.1007/s11258-007-9309-6
- 805 Garon-Labreque MÉ, Léveillé-Bourret É, Higgins K and Sonnentag O. 2015. Additions to the boreal flora of the Northwest Territories with a preliminary vascular flora of Scotty Creek. *Can. Field-Nat.* 129, 349–67. dx.doi.org/10.22621/cfn.v129i4.1757
- Gibson, C.M., Chasmer, L.E., Thompson, D.K., Quinton, W.L., Flannigan, M.D., & Olefeldt, D. (2018). Wildfire as a major driver of recent permafrost thaw in boreal peatlands, *Nature Communications*, 9, 3041. doi.org/10.1038/s41467-018-05457-1
- 810 Haynes, K.M., Connon, R.F. & Quinton W.L. (2018). Permafrost thaw induced drying of wetlands at Scotty Creek, NWT, Canada. *Environmental Research Letters*, 13. doi.org/10.1088/1748-9326/aae46c
- Haynes, K.M., Connon, R.F. & Quinton, W.L. (2019). Hydrometeorological measurements in peatland-dominated, discontinuous permafrost at Scotty Creek, Northwest Territories, Canada. *Geosci Data J.*, 6, 85–96. doi.org/10.1002/gdj3.69
- 815 Haynes, K.M., Smart, J., Disher, B., Carpino, O. & Quinton, W.L. (2020). The role of hummocks in re-establishing black spruce forest following permafrost thaw. *Ecohydrology*, DOI: 10.1002/eco.2273.
- 820 Hayashi, M., Quinton, W. L., Pietroniro, A., & Gibson, J. J. (2004). Hydrologic functions of wetlands in a discontinuous permafrost basin indicated by isotopic and chemical signatures. *Journal of Hydrology*, 296, 81-97. doi.org/10.1016/j.jhydrol.2004.03.020
- Helbig, M., Pappas, C. & Sonnentag, O. (2016a). Permafrost thaw and wildfire: Equally important drivers of boreal tree cover changes in the Taiga Plains, Canada. *Geophysical Research Letters*, 43, 1598-1606. doi.org/10.1002/2015GL067193
- 825 Helbig, M., Wischnewski, K., Kljun, N., Chasmer, L.E., Quinton, W.L., Detto, M. & Sonnentag, O. (2016b). Regional atmospheric cooling and wetting effect of permafrost thaw-induced boreal forest loss. *Glob Change Biol*, 22, 4048-4066. doi.org/10.1111/gcb.13348
- 830 Holloway, J.E. & Lewkowicz, A.G. (2019). Half a century of discontinuous permafrost persistence and degradation in western Canada. *Permafrost and Periglac Process.*, 31, 85-96. doi.org/10.1002/ppp.2017
- Hugelius G., Bockheim J.G., Camill P., Elberling B., Grosse G., Harden J.W., Johnson K., Jorgenson T., Koven C.D., Kuhry P., Michaelson G., Mishra U., Palmtag J., Ping C.-L., O'Donnell J., Schirrmeister L., Schuur E.A.G., Sheng Y., Smith L.C., Strauss J. and Yu Z. (2013a). *Earth System Science Data*, 5, 393–402. DOI:10.5194/essd-5-393-2013
- 835 Hugelius, G., Tarnocai, C., Broll, G., Canadell, J. G., Kuhry, P., and Swanson, D. K. (2013b) *Earth System Science Data*, 5, 3–13. DOI:10.5194/essd-5-3-2013
- Iversen, C.M., Childs, J., Norby, R.J., Ontl, T.A., Kolka, R.K., Brice, D.J., McFarlane, K.J. & Hanson, P.J. (2018). Fine-root growth in a forested bog is seasonally dynamic, but shallowly distributed in nutrient-poor peat. *Plant Soil*, 424, 123-143. doi.org/10.1007/s11104-017-3231-z
- 840

- 845 Ketteridge, N., Thompson, D. K., Bombonato, L., Turetsky, M. R., Benscoter, B. W.,
Waddington, J. M. (2013). The ecohydrology of forested peatlands: simulating the effects
of tree shading on moss evaporation and species composition. *Journal of Geophysical
Research – Biogeosciences*, 118, 422-435. doi.org/10.1002/jgrg.20043
- 850 Kokelj, S.V., Palmer, M.J., Lantz, T.C. & Burn, C.R. (2017). Ground Temperatures and
Permafrost Warming from Forest to Tundra, Tuktoyaktuk Coastlands and Anderson
Plain, NWT, Canada. *Permafrost and Periglacial Processes*, 28, 543– 551.
doi.org/10.1002/ppp.1934
- Korosi, J.B., Thienpont, J.R., Pisaric, M.F.J., deMontigny, P., Perreault, J.T., McDonald, J.,
Simpson, M.J., Armstrong, T., Kokelj, S.V., Smol, J.P., & Blais, J.M. (2017). Broad-
scale lake expansion and flooding inundates essential wood bison habitat, *Nature
Communications*, 8, 14510. doi.org/10.1038/ncomms14510
- 855 Kurylyk, B., Hayashi M., Quinton W., McKenzie J., & Voss C. (2016). Influence of vertical and
lateral heat transfer on permafrost thaw, peatland landscape transition, and groundwater
flow. *Water Resources Research*, 52 (2), 1286-1305. doi.org/10.1002/2015WR018057
- 860 Kwong, J. T. & Gan, T. Y. (1994). Northward migration of permafrost along the Mackenzie
Highway and climatic warming. *Climate Change*, 26, 399-419.
doi.org/10.1007/BF01094404
- Lieffers, V. J. & Rothwell, R.L. (1987). Rooting of peatland black spruce and tamarack in
relation to depth of water table. *Canadian J. Bot.* 65, 817-821.
- Loisel, J. & Yu, Z. (2013). Surface vegetation patterning controls carbon accumulation in
peatlands. *Geophysical Research Letters*, 40, 5508-5513. doi.org/10.1002/grl.50744
- 865 McKenzie, J. M., & Voss, C. I.(2013). Permafrost thaw in a nested groundwater-flow system.
Hydrogeology Journal, 21(1), 299–316.
- Mekis, É & Vincent, L.A. (2011). An overview of the second generation adjusted daily
precipitation dataset for trend analysis in Canada. *Atmosphere-Ocean*, 49(2), 163-177.
doi.org/10.1080/07055900.2011.583910
- 870 NWWG. 1988. Wetlands of Canada. Ecological Land Classification Series, no. 24. Sustainable
Development Branch, Environment Canada, Polyscience Publications Inc., Ottawa,
Ontario Montreal, Quebec.
- Natural Resources Canada (2017). Wooded areas, saturated soils and landscape in Canada –
CanVec series – Land features. Available at:
875 <https://open.canada.ca/data/en/dataset/80aa8ec6-4947-48de-bc9c-7d09d48b4cad>
(Accessed July 10, 2019)
- 880 Olefeldt, D., Goswami, S., Grosse, G., Hayes, D., Hugelius, G., Kuhry, P., McGuire, A.D.,
Romanovsky, V.E., Sannel, A.B.K., Schuur, E.A.G. & Turetsky, M.R. (2016).
Circumpolar distribution and carbon storage of thermokarst landscapes, *Nature
Communications*, 7, 13043. doi.org/10.1038/ncomms13043
- Olefeldt, D., Persson, A., Turetsky, M.R. (2014). Influence of the permafrost boundary on
dissolved organic matter characteristics in rivers within the Boreal and Taiga plains of
western Canada. *Environ. Res. Lett.* 9 035005. doi:10.1088/1748-9326/9/3/035005

- 885 Overland, J.E., Hanna, E., Hanssen-Bauer, I., Kim, S.J., Walsh, J.E., Wang, M., Bhatt, U.S.,
Thoman, R.L., & Ballinger, T.J. (2019): Surface Air Temperature. Arctic Report Card
2019, J. Richter-Menge, M. L. Druckenmiller, and M. Jeffries, Eds.,
<http://www.arctic.noaa.gov/Report-Card>.
- 890 Pelletier, N. Talbot, J., Olefeldt, D., Turetsky, M., Blodau, C., Sonnentag, O., Quinton, W.L.
(2017). Influence of Holocene permafrost aggradation and thaw on the paleoecology and
carbon storage of a peatland complex in northwestern Canada. *Holocene*, 27, 1391–1405.
doi.org/10.1177/0959683617693899
- 895 Pomeroy, J.W., Toth, B., Granger R.J., Hedstrom N.R., & Essery R.L.H. (2003). Variation in
surface energetics during snowmelt in a subarctic mountain catchment. *Journal of
Hydromet.*, 4, 702-719. DOI: 10.1175/1525-7541(2003)004<0702:VISED>2.0.CO;2
- Porter, T.J., Schoenemann, S.W., Davies, L.J. *et al.* Recent summer warming in
northwestern Canada exceeds the Holocene thermal maximum. *Nat Commun* 10, 1631
(2019). <https://doi.org/10.1038/s41467-019-09622-y>
- 900 Quinton, W., Berg, A., Braverman, M., Carpino, O., Chasmer, L., Connon, R., Craig, J., Devoie,
É., Hayashi, M., Haynes, K., Olefeldt, D., Pietroniro, A., Rezanezhad, F., Schincariol, R.,
and Sonnentag, O. (2019). A synthesis of three decades of hydrological research at Scotty
Creek, NWT, Canada, *Hydrol. Earth Syst. Sci.*, 23, 2015-2039. [doi.org/10.5194/hess-23-
2015-2019](https://doi.org/10.5194/hess-23-2015-2019)
- 905 Quinton, W. L. & Carey, S. K. (2008). Towards an energy-based runoff generation theory for
tundra landscapes, *Hydrological Processes.*, 22. DOI: 10.1002/hyp.7164
- Quinton, W. L., Hayashi, M., & Chasmer, L. E. (2009). Peatland hydrology of discontinuous
permafrost in the Northwest Territories: overview and synthesis. *Canadian Water
Resources Journal*, 34(4), 311–328. doi.org/10.4296/cwrj3404311
- 910 Quinton, W., Hayashi, M., & Chasmer, L. (2011). Permafrost-thaw-induced land- cover change
in the Canadian subarctic: Implications for water resources. *Hydrological Processes*, 25,
152-158. doi.org/10.1002/hyp.7894
- Quinton, W.L., Hayashi, M. & Pietroniro, A. (2003), Connectivity and storage functions of
channel fens and flat bogs in northern basins. *Hydrol. Process.*, 17, 3665-3684.
doi.org/10.1002/hyp.1369
- 915 Robinson, S.D., 2002. Peatlands of the Mackenzie Valley: Permafrost, Fire, and Carbon
Accumulation. In: Long-Term Dynamics...Z.C. Yu *et al.* (eds.). Proc. of Int. Workshop
on Carbon Dynamics of Forested Peatlands: Knowledge Gaps, Uncertainty and
Modelling Approaches. 23-24 March, 2001, Edmonton, Canada, 21-24.
- 920 Robinson, S. D., & Moore, T. R. (2000). The influence of permafrost and fire upon carbon
accumulation in high boreal peatlands, Northwest Territories, Canada. *Arctic, Antarctic,
and Alpine Research*, 32(2), 155–166. doi.org/10.1080/15230430.2000.12003351
- Rowland, J.C., C. E. Jones G. Altmann R. Bryan B. T. Crosby L. D. Hinzman D. L. Kane D.
M. Lawrence A. Mancino P. Marsh J. P. McNamara V. E. Romanvosky H. Toniolo
B. J. Travis E. Trochim C. J. Wilson G. L. Geernaert, 2010. Arctic Landscapes in

- 925 Transition: Responses to Thawing Permafrost. Vol. 91, no. 26, pp. 229-230.
<https://doi.org/10.1029/2010EO260001>
- Schuur, T., (2019) Permafrost and the Global Carbon Cycle. Arctic Report Card 2019, J. Richter-Menge, M. L. Druckenmiller, and M. Jeffries, Eds., <http://www.arctic.noaa.gov/Report-Card>.
- 930 Smith, S.L., Burgess, M.M., Riseborough, D. & Nixon, F.M. (2005). Recent trends from Canadian permafrost thermal monitoring network sites. *Permafrost and Periglac. Process.* 16, 19-30. DOI: 10.1002/ppp.511
- Smith, S.L., Burgess, M.M., Riseborough, D.W. (2008). Ground temperature and thaw settlement in frozen peatlands along the Norman Wells pipeline corridor, NWT Canada:
 935 22 years monitoring. *Ninth International Conference on Permafrost*, 1665-1670.
- Smith, S.L. & Riseborough, D.W. (2010). Modelling the thermal response of permafrost terrain to right-of-way disturbance and climate warming. *Cold Regions Science and Technology*, 60, 92-103. <https://doi.org/10.1016/j.coldregions.2009.08.009>
- St. Jacques, J.M. & Sauchyn, D.J. (2009). Increasing winter baseflow and mean annual
 940 streamflow from possible permafrost thawing in the Northwest Territories, Canada. *Geophysics Research Letters* 36. doi.org/10.1029/2008GL035822
- Stofferahn, E., Fisher, J.B., Haynes, D.J., Schwalm, C.R., Huntzinger, D.N., Hantson, W., Poulter, B., Zhang, Z. (2019). The Arctic-Boreal vulnerability experiment model benchmarking system. *Environ. Res. Lett.* 14 055002. <https://doi.org/10.1088/1748-9326/ab10fa>
- 945 Tarnocai, C. (2009) The impact of climate change on Canadian peatlands *Can. WaterRes. J.*, 34, 453-66. doi.org/10.4296/cwrj3404453
- Thie, J. (1974). Distribution and thawing of permafrost in the southern part of the discontinuous permafrost zone in Manitoba. *Arctic Journal of the Arctic Institute of North America*, 34(3), 189-200. doi.org/10.14430/arctic2873
- 950 Treat, C.C. & Jones, M.C. (2018). Near-surface permafrost aggradation in Northern Hemisphere peatlands shows regional and global trends during the past 6000 years. *The Holocene*, 28(6):998-1010. doi:10.1177/0959683617752858
- Vincent, L.A., Wang, X.L., Milewska, E.J., Wan, H., Yang, F., & Swail, V. (2012). A second
 955 generation of homogenized Canadian monthly surface air temperature for climate trend analysis. *Journal of Geophysical Research*, 117, pp 13. doi.org/10.1029/2012JD017859
- Vincent, L., Zhang, X., Brown, R., Feng, Y., Mekis, E., Milewska, E., Wan, H., & Wang, X. (2015). Observed trends in Canada's climate and influence of low-frequency variability modes, *Journal of Climate*, 28. doi.org/10.1175/JCLI-D-14-00697.1
- 960 Vitt, D. H., Halsey, L. A., & Zoltai, S. C. (1994). The bog landcovers of continental Western Canada in relation to climate and permafrost patterns. *Arctic and Alpine Research*, 26(1), 1– 13. DOI: 10.1080/00040851.1994.12003032
- Walvoord, M. and B. Kurylyk, 2016. Hydrologic Impacts of Thawing Permafrost - A Review. *Vadose Zone Journal*, 15, 6. doi:10.2136/vzj2016.01.0010.

- 965 Walvoord, M.A., Voss, C.I., Ebel, B.A. & Minsley, B.J. (2019) Development of perennial thaw zones in boreal hillslopes enhances potential mobilization of permafrost carbon, *Environ. Res. Lett.* 14. doi.org/10.1088/1748-9326/aaf0cc
- Warren, R.K., Pappas, C., Helbig, M., Chasmer, L.E., Berg, A.A., Baltzer, J.L., Quinton, W.L., & Sonnetag, O. (2018). Minor contribution of overstory transpiration to landscape evapotranspiration in boreal permafrost peatlands, *Ecohydrology* 11, 1975. doi.org/10.1002/eco.1975
- 970 Webster, C. Rutter, N., Zahnner, F. & Jonas, T. (2016). Measurement of Incoming Radiation below Forest Canopies: A Comparison of Different Radiometer Configurations. *J. Hydrometeor.* 17, 853–864. doi.org/10.1175/JHM-D-15-0125.1
- 975 Wright, N., Hayashi, M., & Quinton, W. (2009). Spatial and temporal variations in active layer thawing and their implication on runoff generation in peat-covered permafrost terrain. *Water Resources Research*, 45(5). doi.org/10.1029/2008WR006880
- Zoltai, S. C., & Tarnocai, C. (1975). Perennially frozen peatlands in the Western Arctic and Subarctic of Canada. *Canadian Journal of Earth Science*, 12, 28–43. doi.org/10.1139/e75-004
- 980 Zoltai, S. C. (1993). Cyclic development of permafrost in the peatlands of Northwestern Alberta, Canada. *Arctic Alpine Research*, 25, 240–6. DOI: 10.1080/00040851.1993.12003011